Evaluation of surface roughness parameters in agricultural soils with different tillage conditions using a laser profile meter

Alex Martinez-Agirre*, Jesús Álvarez-Mozos and Rafael Giménez

Public University of Navarre, Dept. of Projects and Rural Engineering. Campus Arrosadia, 31006 Pamplona, Spain

*Corresponding Author: Phone: (34) 948168937. e-mail: alejandro.mda@unavarra.es

Abstract

Surface roughness crucially affects the hydrological and erosive behaviours of soils. In agricultural areas surface roughness is directly related to tillage, whose action strongly affects the key physical properties of soils and determines the occurrence and fate of several processes (e.g., surface storage, infiltration, etc.). The characterisation of surface roughness as a result of tillage operations is not straightforward, and numerous parameters and indices have been proposed for quantifying it. In this article, a database of 164 profiles (each 5 m long), measured in 5 different roughness classes, was analysed. Four roughness classes corresponded to typical tillage operations (i.e., mouldboard, harrow, seedbed, etc.), and the fifth represented a seedbed soil that was subject to rainfall. The aim of the research was to evaluate and select the surface roughness parameters that best characterised and quantified the surface roughness caused by typical tillage operations. In total, 21 roughness parameters (divided into 4 categories) were assessed. The parameters that best separated and characterised the different roughness classes were the limiting elevation difference (*LD)* and the Mean Upslope Depression index (*MUD*); however, the parameters most sensitive to rainfall action on seedbed soils were limiting slope (*LS*) and the crossover lengths measured with the semivariogram method (l_{SMV}) and

the root mean square method (l_{RMS}). Many parameters had high degrees of correlation with each other, and therefore gave almost identical information. The results of this study may contribute to the understanding of the surface roughness phenomenon and its parameterisation in agricultural soils.

Keywords: surface roughness, roughness parameters, agricultural soils, tillage

1. Introduction

Surface roughness is a key element in the hydrological and erosive behaviour of soils (Helming at al., 1998), and as a soil-atmosphere frontier, plays an important role in many processes, such as infiltration, runoff, the detachment of soil due to water or wind, gas exchange, evaporation and heat fluxes (Huang and Bradford, 1992).

Depending on the order of magnitude of the soil surface elevation variations, and on the spatial arrangement of its microforms, surface roughness can be classified into different categories (Römkens and Wang, 1986): (1) Variations in the soil`s microrelief due to its individual particles and/or microaggregates (variations of the order of 1 mm, but up to 2 mm). (2) Variations in the surface generated by soil clods caused by agricultural practices (variations of the order of 100 mm, but up to 200 mm); these two roughness types are considered random and isotropic (i.e., uniform in all directions). (3) Roughness due to the systematic differences in elevation (i.e., rows or furrows) caused by tillage implements (variations between 100-200 mm); these forms are one-directional and this component is, therefore, oriented or anisotropic. (4) Roughness due to the macroforms of the terrain (of the order of several meters), which together define the topography of the landscape; these elevation variations are usually non-directional. Although the classification of Römkens and Wang (1986) associated the effect of tillage with an oriented type of roughness (category 3), it is understood that random roughness (categories 1 and 2) is also affected, to a greater or lesser extent, by tillage.

The order of magnitude in the elevation variations of the two (or three) first roughness types is lower than the spatial resolution of the digital elevation models that are conventionally used (Govers et al., 2000; Mushkin and Gillespie, 2005). Hence, in order to quantitatively characterise those microforms, it is necessary to take complementary measurements *in situ*, which permit the calculation of different surface roughness parameters or indices.

The parameterisation of the random surface roughness caused by tillage (the first two categories cited above) is not straightforward. Each tillage practices (or implements) causes, in theory, a particular type of microrelief under identical soil conditions (in terms of texture, moisture, density, etc.). Considering the wide range of possible soil conditions, a huge variety of roughness types could be found in agricultural soils immediately after tilling. In addition, soil physical properties, particularly surface roughness, can also be highly variable in space. To further complicate its characterisation, surface roughness also shows a multi-scale nature making any roughness measurement scale-dependent (Zhixiong et al., 2005; Verhoest et al., 2008; Álvarez-Mozos et al., 2011). Finally, the microrelief generated by the different tillage practices is more or less susceptible to change throughout time due to the action of meteorological agents, e.g., precipitation (Dalla Rosa et al., 2012), wind and temperature changes in the low atmosphere (Pardini, 2003), or even animal activity.

Although there are many parameters and indices for quantifying surface roughness (e.g., Helming et al., 1993; Magunda et al., 1997; Kamphorst et al., 2000; Vermang et al., 2013), none work universally and interested scientists/technicians find it difficult to select the most appropriate one for their particular case. The random roughness parameters that are most commonly used in the literature, described in section 2.3, were considered in this study; these parameters can be divided into four groups, following a criterion similar to that of Smith (2014): (1) parameters measuring the vertical dimension of roughness or the magnitude of the elevation variations of the points at the soil surface (vertical parameters), (2) parameters measuring the horizontal dimension of roughness or the relation between the height of a point and that of its neighbours (horizontal parameters), (3) parameters combining both dimensions (combined parameters), and (4) parameters based on fractal theory, which measure self-affinity or the balance between height variations at different spatial scales (fractal parameters).

In light of the above, the aim of this research was to evaluate and select the most appropriate surface roughness parameters to characterise and quantify the surface roughness caused by typical tillage operations.

2. Material and methods

2.1. Test site

Roughness data were taken in 10 agricultural fields, with an extension ranging from 3 ha to 7.3 ha. Fields were located in the experimental hydrological watershed of La Tejería (N42º44’10.6’’ and W1º56’57.2’’) in Navarre (Spain), which has been used in different research works in the past (e.g., Casalí et al., 2008; Álvarez-Mozos et al., 2009; Álvarez-Mozos et al., 2011). Each of the fields was subjected to different tillage operations (see Fig. 1.A-E and Table 1) following the conventional soil preparation calendar in the area. Thus, during the months of September and October, 2004, the obtained data corresponded to soils subjected to primary tillage, i.e., classes Mouldboard Plough (MP), Harrowed Rough (HR), and Harrowed Smooth (HS). In the month of November 2004, soils were sown with cereal crops, representing typical seedbed conditions; this class was referred to as Planted Unmodified (PU). Finally, a final measurement was carried out in March 2005. By this time, seedbed soils had been modified by the action of the rainfall that had occurred since sowing (~250 mm); this class was referred to as Planted Modified (PM). In total, 164 profiles were taken (see Table 1). Profiles were measured in parallel to tillage rows, to reflect the random roughness component.

Insert Figure 1 here

Insert Table 1 here

2.2. Profile measurements

Profiles were taken with a profilometer designed *ad hoc* for roughness measurement (Álvarez-Mozos et al., 2005). This instrument incorporates a laser sensor that measures the vertical distance from a reference bar down to the surface. The laser profilometer (see Fig. 1.F) consists of an aluminium bar with its ends fixed to two tripods. The laser distance meter is located inside a case that moves along the aluminium bar, propelled by a small electric motor. The laser profilometer has a vertical accuracy of 1.25 mm and a measurement interval of 5 mm. The total length of profiles was 5 m, so that in each one there are 1000 height records.

Profiles were processed using a code developed *ad hoc,* consisting of: (1) the correction of the buckling effect on the aluminium bar by detrending profiles with a parabolic curve obtained from a perfect horizontal reference surface, (2) the application of a filter to eliminate the outliers eventually detected in the height records (e.g., plant material) by deleting and interpolating records with height differences larger than 10 cm with the previous and next records, and (3) the correction of terrain slope (i.e., profile detrending) through the subtraction of the linear trend observed in the data (Xingming et al., 2014).

Once this process had been carried out, the profiles were ready for the calculation of the different roughness parameters.

It should be noticed that the data analysed in this study are 2D profiles and that inferences about 3D phenomena (e.g., depression storage) should be made with caution.

2.3. Calculation of roughness parameters

In total, 21 surface roughness parameters were analysed (Table 2); these parameters could be classified into vertical, horizontal, combined, and fractal parameters, as explained in the introduction. Next, each parameter is briefly described; parameter names are highlighted in bold for clarity.

Insert Table 2 here

Random roughness, one of the indices most frequently used to describe surface roughness, was proposed by Allmaras et al. (1966) as the standard deviation of heights after the elevations were transformed to natural logarithms and corrected for slope and tillage tool marks. After Currence and Lovely (1970) showed that the parameter was more sensitive without any logarithmic transformation, most authors (e.g., Bertuzzi et al., 1990; Hansen et al., 1999; Kamphorst et al., 2000) calculate random roughness as the **standard deviation of heights** *(s)* (eq. 1):

$$s = \sqrt{\frac{\sum_{i=1}^{N}(z_i{}^2 - \bar{z}^2)}{N-1}} \quad (1)$$

where N is the number of height records, z_i is the height corresponding to record i, and $\bar{z}$ is the mean height of all the records.

The **correlation length** (l_{ACF}) represents the horizontal component of roughness, i.e., it describes the relative location of heights or the way in which the heights vary along the surface (Ogilvy and Foster, 1989). The correlation length was calculated from the autocorrelation function (eq. 2) (Ulaby et al., 1982):

$$\rho(h) = \frac{\sum_{i=1}^{N(h)} z_i z_{i+h}}{\sum_{i=1}^{N} z_i{}^2} \qquad (2)$$

where $\rho(h)$ is the autocorrelation function, which represents the correlation existing between height z of the point i (z_i) and that of another point located at a lag distance h from it (z_{i+h}), and $N(h)$ is the number of pairs considered in each lag h. The correlation length (l_{ACF}) is then defined arbitrarily as the distance at which the heights of two points on the surface are considered independent; i.e., $\rho(h)$ is equal to $1/e$, so that $\rho(l) = 1/e$. Another parameter extracted from the autocorrelation function is its **initial slope** ($\rho'(0)$), which also provides a measure of the horizontal roughness (Borgeaud et al., 1995), but in this case at a more local scale, i.e., focusing on the height variations of a point with its nearest neighbours. Zribi and Dechambre (2003) proposed **parameter Z_S** as a combination of s and l_{ACF} (eq. 3), and thus accounted for both vertical and horizontal roughness components:

$$Z_s = s^2/l_{ACF} \qquad (3)$$

The concepts of the **limiting elevation difference** (*LD*) and the **limiting slope** (*LS*) were developed to include the spatial aspect of roughness (Linden and Van Doren, 1986). Parameter *LD* supplies information on the characteristics of roughness at long distances, whereas *LS* is used to characterise roughness at short distances (Bertuzzi et al., 1990). The mean absolute-elevation-difference is defined as (eq. 4):

$$\Delta z_h = \sum_{i=1}^{N(h)} \frac{|z_i - z_{i+h}|}{N(h)} \qquad (4)$$

The relationship between Δz_h and the lag distance h was obtained from a hyperbolic linear model defined by (eq. 5):

$$1/\Delta z_h = a + b(1/h) \tag{5}$$

where a and b are the fitting parameters obtained for an arbitrary horizontal distance. After testing different values, and following the recommendation of Linden and Van Doren (1986), this distance was set to 20 cm. Parameter *LD* (eq. 6) determines the shape of the variogram, assumed to follow a hyperbolic function:

$$LD = 1/a \tag{6}$$

Parameter *LS* (eq. 7) is the original variogram slope (Kamphorst et al. 2000), given by:

$$LS = 1/b \tag{7}$$

Linden et al. (1988) proposed a third parameter that was obtained as a combination of parameters *LD* and *LS*, called **parameter *Q*** (eq. 8). This parameter can be considered a combined roughness parameter.

$$Q = (LD \cdot LS)^{1/2} \tag{8}$$

The semivariogram represents how height data are related to distance. The semivariance function depending on the lag *h* can be calculated as:

$$\gamma(h) = \frac{1}{2N(h)} \sum_{i=1}^{N(h)} [z_{i+h} - z_i]^2 \tag{9}$$

Once the experimental semivariogram was calculated, a spherical model was fitted to it (Vázquez et al., 2009; Croft et al., 2013):

$$\gamma(h) = \begin{cases} c_1 \left[1.5\frac{h}{h_a} - 0.5\left(\frac{h}{h_a}\right)^3\right] + c_0 & ; h \leq h_a \\ c_1 + c_0 & ; h > h_a \end{cases} \tag{10}$$

where h_a is the Range, c_1 is the Sill, and c_0 is the Nugget. After testing different values, 100 cm of maximum lag distance was deemed sufficient to accurately fit the spherical model to the experimental semivariogram. ***Sill*** represents the value of $\gamma(h)$ where the fitted model reaches the plateau, and ***Range*** is the distance at which the *Sill* is found. No nugget effect was taken into account (Vermang et al., 2013). Both *Sill* and *Range* have been frequently used as soil surface roughness indices (e.g., Helming et al., 1993; Vázquez et al., 2009; Croft et al., 2009, Croft et al., 2013; Vermang et al., 2013).

Parameter *MIF* (eq. 11) was formulated by Römkens and Wang (1986) with the aim of quantitatively describing surface roughness. This dimensionless parameter represents the integrated effect of the **peak frequency** (*F*) and the **microrelief index** (*MI*), and it is defined arbitrarily as:

$$MIF = MI \cdot F \tag{11}$$

where *MI* represents the area per unit of length between the measured surface profile and the regression line of least squares through all measured elevations on a transect (Römkens and Wang, 1986), and *F* is the number of peaks (i.e., points with higher elevations than their neighbours on both sides) per unit of length of the profile. Parameters *MI* and *F* (eq. 11) are evaluated separately as descriptive parameters of vertical and horizontal roughness, respectively.

The **Mean Upslope Depression index** (*MUD*) (eq. 12) was specifically developed to predict surface storage capacity (Hansen et al., 1999). The *MUD* is based on the elevation differences $(z_i - z_{i+h})$ between a reference point *i* and another *i*+*h* on a line segment positioned upslope from the reference point. Within each line segment, the calculation procedure is iterated for a number of sub-segments, each time taking a new upslope point as the reference point (Hansen et al., 1999):

$$MUD = \sum_{i=1}^{m}\left(\sum_{j=1}^{n}\frac{\Delta z}{n}\right)/m \begin{cases}\Delta z = z_i - z_{i+h}\,; z_i \geq z_{i+h}\\ \Delta z = 0 \qquad\quad ; z_i < z_{i+h}\end{cases} \tag{12}$$

where n is the number of points in a line sub-segment and m is the number of line sub-segments. In Hansen et al. (1999), no particular segment length was recommended, but they considered a 30-cm length for their conditions. In our case, after testing different values, a segment length of 20 cm was selected.

Tortuosity is a roughness index based on the ratio of the surface profile perimeter length (L_1) and its horizontal projection (L_0). Although variants do exist (e.g., Boiffin, 1984; Planchon et al., 1998), the present study used the tortuosity index of Saleh (T_S) (eq. 13) (Saleh et al., 1993):

$$T_S = 100 \cdot \frac{(L_1 - L_0)}{L_1} \tag{13}$$

Different methods have been used to calculate the **fractal dimension** (and in some cases the **crossover length**), which characterises the self-affinity of surface roughness profiles. The **semivariogram method** (SMV) was introduced to study the variability of soil properties and subsequently used to quantify roughness (Burrough, 1983a,b; Armstrong, 1986; Huang and Bradford, 1992; Vidal Vázquez et al., 2005; Chi et al., 2012; Vermang et al., 2013). The first step in the estimation of the fractal dimension is the calculation of the experimental semivariogram (eq. 9) (Vidal Vázquez et al., 2005). Assuming a fractal Brownian motion (*fBm*) model, the experimental semivariogram can be described as a function of the lag (Eq. 14):

$$\gamma(h) = l^{1-H} h^H \tag{14}$$

where l is the crossover length and H is the Hurst coefficient. After a log-log transformation of eq. 14, H can be estimated as the slope of the semivariance versus the lag distance. When applied to surface roughness profiles, the logarithmic transformation normally yields a curved trend rather than a line, thus revealing a multi-fractal nature (Vidal Vázquez et al., 2005; Moreno et al., 2008). In this study, only the fractality of the first stretch (where the linear assumption holds) was measured. For that purpose, a maximum lag distance of 10 cm was considered because it provided a good fit to the linear trend in all the profiles. Afterward, the Hurst coefficient was related to the fractal dimension as follows (Smith, 2014) (eq. 15):

$$D_{SMV} = 1 + d - H = 2 - H \qquad (15)$$

where d is the Euclidean dimension of the system (i.e., 1 for profiles, 2 for surfaces, etc.). Further, the crossover length (l_{SMV}) (eq. 16) can be calculated as follows (Huang and Bradford, 1992):

$$l_{SMV} = exp\left[\frac{a_{SMV}}{(2-2H)}\right] \qquad (16)$$

where a_{SMV} is the intercept of the linear trend fitted to the first stretch of the semivariogram.

The **root mean square method** (RMS) is based on the evaluation of the root mean square deviation of elevation values for increasing lag distances, and it has been used in different studies (Malinverno, 1990; Gallant et al., 1994; Moreira et al., 1994; Vidal Vázquez et al., 2005). The average RMS values for increasing lag distances (h) are calculated as (Vidal Vázquez et al., 2005):

$$\overline{W}(h) = \frac{1}{n_h}\sum_{u=1}^{n_h}\left\{\frac{1}{n}\sum_{i\in h}[z_i - \bar{z}_h]^2\right\}^{1/2} \qquad (17)$$

where n_h is the total number of lags of size h and $\bar{z}_h$ represents the average elevation values for all points of each lag. As in the semivariogram method, the slope of the logarithmic transformation of $\overline{W}(h)$ gives an estimation of the Hurst coefficient, which enables the calculation of the fractal dimension (D_{RMS}) and the crossover length (l_{RMS}) (eq. 15 and 16).

The estimation of the fractal dimension by the **box counting method** (BC) is motivated by the scale law defined by Mandelbrot (1977):

$$D(r) = \frac{\log(N_r)}{\log(1/r)} \qquad (18)$$

where N_r stands for the minimum number of boxes of a width r that can cover the object (i.e., surface profile). The basic idea is simple since the profile to be studied is initially covered by a single box. That box is divided into 4 quadrants, and the number of quadrants required to cover the profile are counted. Then, each quadrant is divided into another four sub-quadrants, and this division goes on until the width of the boxes reaches the resolution of the data, counting the number of cells required to cover the profile in each step (Gneiting et al., 2012). Function $D(r)$ is transformed into logarithms and fitted to a regression line, from whose slope (α) the fractal dimension D_{BC} (eq. 19) (Liang et al., 2012) is obtained:

$$D_{BC} = -\alpha \qquad (19)$$

A further technique used to determine the Hurst coefficient, and hence the fractal dimension, is the **power spectrum method** (PS) (Gneiting et al., 2012). This estimator is based on the spectral density function $S(v)$ for a stationary stochastic process, obtained by the fast Fourier transform (FFT), which depicts how the roughness is distributed in components of different frequencies (v). The Hurst coefficient is obtained through the regression line of the logarithmic transformation of function $S(v)$, and thereafter the fractal dimension (D_{PS}) (eq. 15).

Finally, the **rescaled range method** (RS) (Liu and Molz, 1996; Liang et. al, 2012) was also used, which is based on calculating the fitted range R in terms of the lag distance h:

$$R(h) = R_a/s(h) \qquad (20)$$

where R_a is the sum of the absolute values of the largest positive and negative deviations of lag points from its trend line, and $s(h)$ is the standard deviation of each lag. As in the previous cases, to obtain the Hurst coefficient, a linear regression of the logarithmic transformation of $R(h)$ is made, from which the fractal dimension (D_{RS}) (eq. 15) is obtained.

2.4. Parameter evaluation

2.4.1. Descriptive analysis

To assess the different parameters, first, the different roughness classes were visually analysed. The box plots generated by each of the parameters per roughness class were also visually analysed.

2.4.2. Separability analysis

The evaluated roughness parameters did not necessarily follow Gaussian probability distribution functions, since they might have asymmetric distributions. Furthermore, the different roughness classes did not necessarily have comparable variances. Hence, the comparison of parameters and classes could not rely on classic statistical tools, such as the analysis of variance (requiring Normality and homoscedasticity), and thus the separability analysis was used to select the most suitable parameters for the characterisation of different roughness classes. Separability, or dissimilarity, is a statistical metric that quantifies how different two sets of data are; it can be evaluated by computing different statistical distance measures (e.g., Divergence, Bhattacharyya distance, etc.). In this study, the Jeffries-Matusita Distance (D_{JM}) (Swain and King, 1973) was used, which was calculated for each parameter and pair of roughness classes. D_{JM} (eq. 21) has been frequently used to analyse similarity and feature selection processes, and a good number of studies recommend its use (e.g., Bruzzone et al., 1995; D'Urso and Menenti, 1996):

$$D_{JM} = \int \left[\left(\sqrt{f(x)} - \sqrt{g(x)} \right)^2 \right] dx \qquad (21)$$

where D_{JM} is the distance between classes $f(x)$ and $g(x)$ measured by the parameter x. D_{JM} has a range of variability between 0 and 2, i.e., 0 means $f(x)$ and $g(x)$ completely overlap and 2 means they are completely separable. Values below 1 can be considered of poor separability, whereas values from 1-1.5 corresponds to moderate separability, and 1.5-2 to high separability (Skriver, 2007). By using this analysis, we aimed to quantify the ability of the different parameters to discriminate between different roughness classes.

2.4.3. Correlation analysis

A correlation analysis was performed to study the relationships between the different roughness parameters. For this purpose, the Spearman correlation coefficient (R) was calculated, which is particularly indicated for detecting any type of monotonic relationship.

3. Results

3.1. Descriptive analysis

Roughness class MP presented a higher range of variation in its profile elevations (i.e., vertical roughness) as a result of the presence of soil clods of up to 10 cm in size, with no clear spatial pattern or arrangement (Fig. 2). Visually, classes HR and HS did not exhibit such a large vertical roughness (which was smaller in HS than in HR), but their horizontal roughness seemed greater than in MP, i.e., displaying more serrated profiles. Classes PU and PM showed an even smaller range of vertical variation, and although PU had a high horizontal roughness, the smoothing effect of the rain, which translated into a lesser horizontal roughness, could be clearly seen in PM. In this first visual analysis, they could be ranked –as we understand– in an increasing order of roughness, as follows: $PM<PU<HS<HR<MP$.

Insert Figure 2 here

3.2. Parameters per roughness class

The behaviour of the different parameters in terms of the roughness classes were analysed using boxplots (Fig. 3). In the vertical parameters the mean class values increased with the roughness, which could be visually observed (Fig. 2). Furthermore, the variability of each class increased as its roughness did, with a minimum variability for classes PM and PU, followed by HS and HR, and with a maximum variability for MP. All in all, different types of tillage (i.e., classes PU, HS, HR, and MP) could be differentiated with relative clarity. The effect of rainfall lowered class PM's values, compared to PU, in most vertical parameters, but their differences were rather small and both classes overlapped to a certain degree.

Insert Figure 3 here

Horizontal parameters did not exhibit the same trend as the vertical ones (Fig. 3). Regarding the variability per class, different patterns were observed for the different parameters, although MP was less variable than the other classes in all parameters. Parameters l_{ACF} and *Range* behaved similarly, with comparable values for the different classes and many outliers especially in the least rough classes (i.e., PM and PU). Parameters $\rho'(0)$ and F followed a similar trend, showing a moderate differentiation between classes PU, HS, HR, and MP; however, the action of precipitation modified that trend and made class PM take lower $\rho'(0)$ and F values than PU, indicating a higher correlation between the surface elevations. Finally, parameter *LS* took increasing values for increasing roughness conditions (i.e., PU, HS, HR, and MP), but there was a high overlap between classes; nevertheless, this parameter seemed to clearly differentiate PM from the other classes.

The combined parameters followed a trend similar to the vertical parameters (Fig. 3), i.e., their values increased with increasing roughness, but the combine parameters did not have the same marked difference in parameter variability than the vertical parameters did, at least not in all cases (see parameters Q and T_S in Fig. 3). Parameters *MIF* and *MUD*, and to a lesser extent Z_S, did behave very similarly to the vertical ones, with increases in variability as roughness increased; however, parameter Q did not follow this behaviour, as it had a very similar variability in all the classes. Finally, parameter T_S followed a completely different pattern, with a good separation between classes PM and PU but minor differences between the rest.

Regarding fractal parameters, the D values calculated with different techniques behaved similarly, although their absolute values differed slightly (Fig. 3); their performance resembled that of parameter $\rho'(0)$. This pattern indicates a more self-affine behaviour as tillage classes increased in roughness, although the precipitation effect modified that tendency. The variability of the fractal dimensions was rather homogeneous for all the classes, but the crossover lengths behaved completely differently. Parameter l_{SMV} followed a very similar trend to the mixed parameters Q and *MUD*, with incrementing values for roughness classes, and a very homogeneous variability for all of them. Meanwhile, parameter l_{RMS} was similar to the horizontal parameter *LS*, with similar values for most tillage classes, but with a clear differentiation of class PM.

3.3. Separability between roughness classes

The vertical parameters and the combined parameters *MUD* and *Q* showed better mean separability with D_{JM} values >1 (Table 3). More precisely, parameters *LD* and *MUD* were those with a higher mean separability (D_{JM}~1.25). The rest of the combined parameters (*MIF*, Z_S and T_S) offered moderate separabilities (D_{JM}~0.9). The horizontal parameters displayed somewhat lower mean separabilities, with D_{JM} values of 0.6-0.7, but in the case of l_{ACF} and *Range*, D_{JM} did not reach 0.3. Lastly, the fractal dimensions calculated with different techniques followed similar patterns, although their mean separabilities varied significantly, from 0.92 (D_{RMS}) to 0.52 (D_{RS}), though the crossover lengths behaved differently. Parameter l_{SMV} ended up reaching a higher separability than 1, while parameter l_{RMS} hardly exceeded the mean separability of 0.4.

Insert Table 3 here

The vertical parameters had the highest separability values between classes PU, HS, HR, and MP, especially parameter *LD*, but none of the vertical parameters was particularly successful at detecting rainfall smoothening, i.e., separating PM and PU, since in no case did D_{JM} reach values above 0.4 for these two classes. Separability values between neighbouring tillage classes (i.e., PU vs. HS, HS vs. HR, and HR vs. MP) were not high for any of the vertical parameters; *Sill* and *LD* functioned best in these cases. For horizontal parameters, separability between class pairs was generally lower than for vertical parameters. Nevertheless, the highest D_{JM} value between classes PM and PU was obtained by parameter *LS* with a value ~0.9. The behaviour of the combined parameters, once more, was similar to the vertical ones, offering separabilities comparable to those, especially for parameters *MUD* and *Q*. Regarding the separation between classes PM and PU, better separabilities were obtained than with the vertical parameters (especially for T_S, Z_S, and *Q*), although still lower than those of *LS*. In addition, parameters *Q*, *MUD*, and T_S offered the highest separabilities between PM and classes HS, HR, and MP. Lastly, regarding fractal parameters, although the different dimensions did not generally exhibit high separabilities, D_{RMS} had some of the highest separabilities between PU and classes HR and MP and between HS and HR and MP, and D_{BC} had the highest separability between classes PU and MP. Regarding the crossover lengths, although the separability between the different tillage types (PU, HS, HR, and MP) was not high, the good separability obtained between class PM and the rest was highly noteworthy (especially for l_{SMV}).

3.4. Parameter correlation

With regard to the correlations between parameters of one type, the vertical parameters were highly correlated with each other, with R~0.9 (Fig. 4); however, the horizontal parameters showed more heterogeneous behaviour with different R values. Parameters l_{ACF} and *Range* had a good correlation (R~0.85), as did $\rho'(0)$ with F, l_{ACF}, and *Range* (although slightly lower, R~0.6), but the other parameters had relatively low correlations. Parameter *LS,* in general, had low correlations with the rest of the horizontal parameters. On the other hand, mixed parameters showed quite homogeneous behaviour with high correlations (R~0.9) with each other, but a little lower for Z_S and *MIF* (R~0.75). Finally, the different fractal dimensions showed high correlations between each other (R≥0.8), except for parameter D_{RS} (R~0.6). The crossover lengths (l_{SMV} and l_{RMS}) were only moderately correlated (R~0.6).

Insert Figure 4 here

Overall, vertical parameters correlated well with mixed ones (R≥0.8), except for Z_S and T_S, which had somewhat lower correlations (R~0.6). A negative correlation was found between the vertical parameters and fractal dimensions, although they measure different phenomena; this would indicate that the greater the vertical roughness, the more self-affine a surface is. The crossover lengths (l_{SMV} and l_{RMS}) presented a disparate behaviour. Although l_{SMV} had a good correlation with the different fractal dimensions (negative correlation), *F* (negative correlation), and most vertical and combined parameters, l_{RMS} had no correlations with the different fractal dimensions and lower correlations than l_{SMV} with the vertical and combined parameters. In both cases, the correlation with parameter *LS* was high, especially in the case of l_{RMS} (R≥0.9).

4. Discussion

4.1. Differentiation between tillage types

The values of *s* and *LD* obtained for the different classes are comparable to those reported in the literature for similar conditions (e.g., Zobeck and Onstad, 1987; Helming et al., 1993; Arvidsson and Bolenius, 2006; Bauer et al., 2015). In the absence of significant changes caused by the rainfall, *s* and *LD* have been successfully related to the size of soil clods and then proposed as good indices for distinguishing different tillage types (Helming et al., 1993; Eltz and Norton, 1997; Magunda et al., 1997; Kamphorst et al., 2000; Vermang et al.. 2013; Bauer et al., 2015). The values of *Sill* obtained here were considerably higher (although within the range of variation) than those reported by Helming et al. (1993) and Vermang et al. (2013), partly because their experiments were carried out using artificial roughness and because of the measurement scale.

Regarding the horizontal parameters, there is no agreement in the literature. For instance, several authors reported increasing values of l_{ACF} for increasing roughness conditions (Davidson et al., 2003; Baghdadi et al., 2008), while others observed more similar behaviour to that obtained here, with no clear differences between roughness classes (Álvarez-Mozos et al., 2005; Verhoest et al., 2008). The *Range* values obtained in this study were, in general, higher (although within the range of variation) than those reported by other authors (Helming et al., 1993; Vermang et al., 2013), but with an important overlap between classes and frequent outliers. Parameters l_{ACF} and *Range* were obtained using different techniques but represent analogous concepts (Vidal Vázquez et al., 2005), and this is corroborated by the results presented here. Parameters $\rho'(0)$ and F were the horizontal parameters that best differentiated tillage classes; this is due to the geometry of the microforms presented in the smooth classes and the macroforms presented in the roughest classes, since the smaller the size of the clods, the more parameter F increased (Bertuzzi et al., 1990). This same phenomenon explains that the reason that $\rho'(0)$ took lower values in the roughest classes was due to the presence of macroforms, which made the autocorrelation function descend more gently in these classes, whereas it did so more abruptly in smoother tillage classes with greater microform presence.

On the other hand, the combined parameters have been rarely used as an approach to separate tillage types. Baghdadi et al. (2008) mentioned that parameter Z_S took on values of <0.1 cm for smooth soils and >0.1 cm for ploughed ones, but did not investigate different tillage practices in greater detail. Zribi and Dechambre (2003) found a direct correlation between the values of Z_S and the clod's size; they reported a variation range of Z_S between 0.07 cm and 1.93 cm for agricultural soils. This trend agrees with our results, although we observed considerable overlapping between similar tillage classes and a slightly narrower range of values. On the other hand, *MIF* appeared to be good parameter to separate different tillage classes (Lehrsch et al., 1988; Bertuzzi et al., 1990).

In fractal parameters, although some authors found that the values of fractal dimensions and their respective crossover lengths (calculated with different techniques) should be relatively similar (Vidal Vázquez et al., 2005; Vivas Miranda et al., 2002), there is not always an agreement between the values shown in different works. For instance, some authors (e.g., Gallant et al., 1994) found substantial variations between methods. In our case, despite the differences in magnitude, we observed that the behaviour was very similar in the different procedures used. This is in accord (except for the case of l_{RMS}) with Chi et al. (2012), who concluded that, generally, the fractal dimension (parameter *D*) decreased and the crossover length (parameter *l*) increased with the increment of soil clods. Vermang et al. (2013) also reported that the rougher the surface, the lower parameter *D* was.

For all the above, parameter *LD* is recommended to separate the different types of tillage studied in terms of the vertical roughness, parameter $\rho'(0)$ in terms of the horizontal roughness, parameter *MUD* in terms of both properties, and parameter D_{RMS} in terms of its self-affinity.

4.2. Effect of rainfall on the different roughness parameters

Although the values of all the vertical parameters changed after successive rainfalls, those changes were not significant enough to clearly differentiate the precipitation effect (Huang and Bradford, 1992; Vermang et al., 2013). In this sense, Bertuzzi et al. (1990) and Magunda et al. (1997) found that parameters representing the roughness' vertical component were good indicators of roughness at higher scales (and then useful to differentiate tillage types), whereas the horizontal parameters were appropriate at lower scales (and hence suitable to evaluate changes in roughness due to rainfall).

As opposed to the vertical parameters, in Vermang et al. (2013), the values of *Range* and l_{ACF} increased after rainfall events (applied with a rain simulator). Helming et al. (1993) and Croft et al. (2009) also observed an increase in parameter *Range* after rain, which Helming et al. (1993) attributed to the smoothing and broadening of the largest soil clods, and Croft et al. (2009) indicated a higher spatial correlation. From a semivariogram analysis, Helming et al. (1993) and Vermang et al. (2013) observed that, on surfaces with small roughness, rain events gave rise to more erratic *Range* patterns. Our results are in agreement with these trends, since the rainfall led to a reduction in vertical parameter values and increases in the *Range* and l_{ACF} values.

There were other parameters that displayed a greater sensitivity to the effect of rain. Parameter *LS* was the most sensitive to the changes in roughness caused by precipitation, followed by l_{RMS} and l_{SMV} or T_S. Taconet and Ciarletti (2007) concluded that T_S was a more suitable parameter than *s* to detect soil smoothing due to rain. With regard to the fractal dimensions, in contrast to what was observed here, Vermang et al. (2013) reported that parameter *D* increased after rain events in the soils with small roughness, while it decreased in very rough soils. Eltz and Norton (1997) also observed an increase in parameter *D* and a reduction in *l* after precipitation. Further, Vidal Vázquez et al. (2007) and Paz-Ferreiro (2008) found similar behaviour to that seen here, with reductions both in *D* and in *l* after rain.

Some of these variations can be, to some extent, explained if we take into account that rain can either smoothen the roughness, if the sealing processes in the soil are dominant, or increase roughness, if rills or gullies are developed (Vermang et al., 2013). The soils studied here had a single tillage treatment modified by the precipitation (roughness class PM), so that in order to confirm these trends, it would be necessary to carry out similar experiments in all the other treatments.

4.3. Correlation between parameters

Most of our findings are in agreement with previous investigations. We observed a strong correlations between the vertical parameters, such as: *s* and *LD* (Linden and Van Doren, 1986; Bertuzzi et al., 1990; Magunda et al., 1997); *s* and *Sill* (Croft et al., 2013); *LS* and

T_S (Bertuzzi et al., 1990); l_{ACF} and *Range* (Vidal Vázquez et al., 2005); and *s* and D_{SMV} (negative correlation) (Chi et al., 2012). However, some of our results partly disagreed with previous findings, e.g., the lack of correlation between *MIF* and other parameters, such as *s* or T_S (Bertuzzi et al., 1990), or the high correlation between *s and LS* (Magunda et al., 1997).

5. Conclusions

In this study, the most widely used roughness parameters in earth sciences were selected and their ability to discriminate between the different soil roughness classes created by typical tillage operations was evaluated.

Vertical and combined parameters took higher values as tillage became rougher. Horizontal parameters did not show such a clear pattern, with some parameters being rather insensitive to tillage (l_{ACF} and *Range*), and other increasing (*LS*) and some others decreasing ($\rho'(0)$ and *F*) as tillage became rougher. On the contrary, the different fractal dimensions that were tested showed a consistent behaviour, with values decreasing (more auto-affine behaviour) as tillage became rougher. All in all, the best parameters for differentiating and characterising different tillage types were *LD* and *MUD*.

The effect of rainfall was apparent in most parameters. The ones most sensitive to rainfall action were the horizontal parameter *LS*, the crossover lengths (l_{SMV} and l_{RMS}), and, to a lesser extent, the combined parameter T_S.

Many of the evaluated parameters were highly correlated with each other (all the vertical parameters or the combined parameters *Q* and *MUD*) and therefore provided almost identical information. For these, our recommendation is to select the simplest ones (i.e., *s* or *MUD*); however, some parameters showed low correlation values with the rest, since they offered complementary information (i.e., l_{SMV}, LS, or l_{ACF}). These parameters could be interesting depending on the particular application pursued.

It is expected that the results of this study could contribute to the understanding of the surface roughness phenomenon and to its parameterisation in agricultural soils; however, more research is needed to better characterise roughness dynamics due to the action of rainfall.

Acknowledgements

The authors are grateful to the Spanish Minister of Economy and Competitiveness for partly founding this research throw scholarship BES-2012-054521 and project CGL2011-24336.

References

Allmaras, R.R., Burwell, R.E., Larson, W.E., Holt, R.F., 1966. Total porosity and random roughness of the interrow zone as influenced by tillage. USDA Conservation Research Report, 7, 1-14.

Álvarez-Mozos, J., Campo, M.T., Gimenez, R., Casali, J., Leibar, U., 2011. Implications of scale, slope, tillage operation and direction in the estimation of surface depression storage. Soil and Tillage Research 111(2), 142–153.

Álvarez-Mozos, J., Verhoest, N.E.C., Larrañaga, A., Casalí, J., González-Audícana, M., 2009. Influence of surface roughness spatial variability and temporal dynamics on the retrieval of soil moisture from SAR observations. Sensors 9(1), 463–489.

Álvarez-Mozos, J., Casalí, J., González-Audícana, M., Verhoest, N.E.C., 2005. Correlation between ground measured soil moisture and RADARSAT-1 derived backscattering coefficient over an agricultural catchment of Navarre (North of Spain). Biosystems Engineering 92(1), 119–133.

Armstrong, A.C., 1986. On the fractal dimensions of some transient soil properties. Journal of Soil Science 37(4), 641–652.

Arvidsson, J., Bölenius, E., 2006. Effects of soil water content during primary tillage - laser measurements of soil surface changes. Soil and Tillage Research 90(1-2), 222–229.

Baghdadi, N., Zribi, M., Loumagne, C., Ansart, P., Anguela, T., 2008. Analysis of TerraSAR-X data and their sensitivity to soil surface parameters over bare agricultural fields. Remote Sensing of Environment 112(12), 4370–4379.

Bauer, T., Strauss, P., Grims, M., Kamptner, E., Mansberger, R., Spiegel, H., 2015. Long-term agricultural management effects on surface roughness and consolidation of soils. Soil and Tillage Research 151, 28–38.

Bertuzzi, P., Rauws, G., Courault, D., 1990. Testing roughness indices to estimate soil surface roughness changes due to simulated rainfall. Soil and Tillage Research 17(1-2), 87–99.

Boiffin, J., 1984. La dégradation structurale des couches superficielles sous l'action des pluies. Thèse de Docteur Ingénieur, Paris INA-PG, 320pp.

Borgeaud, M., Attema, E., Salgado-Gispert, G., Bellini, A., Noll, J., 1995. Analysis of bare soil surface roughness parameter with ERS-1 SAR data, in: Symposium on the Extraction of Bio and Geophysical Parameters from SAR Data for Land Applications. pp. 307–316.

Bruzzone, L., Roli, F., Serpico, S.B., 1995. Extension of the Jeffreys-Matusita distance to multiclass cases for feature selection. IEEE Transactions on Geoscience and Remote Sensing 33(6), 1318–1321.

Burrough, P.A., 1983a. Multiscale sources of spatial variation in soil. I. The application of fractal concepts to nested levels of soil variation. Journal of Soil Science 34(3), 577–597.

Burrough, P.A., 1983b. Multiscale sources of spatial variation in soil. II. A non-Brownian fractal model and its application in soil survey. Journal of Soil Science 34(3), 599–620.

Casalí, J., Gastesi, R., Álvarez-Mozos, J., De Santisteban, L.M., Lersundi, J.D.V. d., Giménez, R., Larrañaga, A., Goñi, M., Agirre, U., Campo, M.A., López, J.J., Donézar, M., 2008. Runoff, erosion, and water quality of agricultural watersheds in central Navarre (Spain). Agricultural Water Management 95(10), 1111–1128.

Chi, Y., Yang, J., Bogart, D., Chu, X., 2012. Fractal analysis of surface microtopography and its application in understanding hydrologic processes. Transactions of the ASABE 55(5), 1781–1792.

Croft, H., Anderson, K., Brazier, R.E., Kuhn, N.J., 2013. Modeling fine-scale soil surface structure using geostatistics. Water Resources Research 49(4), 1858–1870.

Croft, H., Anderson, K., Kuhn, N.J., 2009. Characterizing soil surface roughness using a combined structural and spectral approach. European Journal of Soil Science 60(3), 431–442.

Currence, H.D., Lovely, W.D., 1970. Analysis of soil surface roughness. Transactions of the American Society of Agricultural Engineers 13(6), 710–714.

Dalla Rosa, J., Cooper, M., Darboux, F., Medeiros, J.C., 2012. Soil roughness evolution in different tillage systems under simulated rainfall using a semivariogram-based index. Soil and Tillage Research 124, 226–232.

Davidson, M.W.J., Mattia, F., Satalino, G., Verhoest, N.E.C., Le Toan, T., Borgeaud, M., Louis, J.M.B., Attema, E., 2003. Joint statistical properties of RMS height and correlation length derived from multisite 1-m roughness measurements. IEEE Transactions on Geoscience and Remote Sensing 41(7), 1651–1658.

D'Urso, G., Menenti, M., 1996. Performance indicators for the statistical evaluation of digital image classifications. ISPRS Journal of Photogrammetry and Remote Sensing 51(2), 78–90.

Eltz, F.L.F., Norton, L.D., 1997. Surface roughness changes as affected by rainfall erosivity, tillage, and canopy cover. Soil Science Society of America Journal 61(6), 1746–1755.
Gallant, J.C., Moore, I.D., Hutchinson, M.F., Gessler, P., 1994. Estimating fractal dimension of profiles: A comparison of methods. Mathematical Geology 26(4), 455–481.
Gneiting, T., Ševcíková, H., Percival, D.B., 2012. Estimators of fractal dimension: Assessing the roughness of time series and spatial data. Statistical Science 27(2), 247–277.
Govers, G., Takken, I., Helming, K., 2000. Soil roughness and overland flow. Agronomie 20(2), 131–146.
Hansen, B., Schjønning, P., Sibbesen, E., 1999. Roughness indices for estimation of depression storage capacity of tilled soil surfaces. Soil and Tillage Research 52(1-2), 103–111.
Helming, K., Römkens, M.J.M., Prasad, S.N., 1998. Surface roughness related processes of runoff and soil loss: A flume study. Soil Science Society of America Journal 62(1), 243–250.
Helming, K., Roth, C.H., Wolf, R., Diestel, H., 1993. Characterization of rainfall - microrelief interactions with runoff using parameters derived from digital elevation models (DEMs). Soil Technology 6(3), 273–286.
Huang, C., Bradford, J.M., 1992. Applications of a laser scanner to quantify soil microtopography. Soil Science Society of America Journal 56(1), 14–21.
Kamphorst, E.C., Jetten, V., Guérif, J., Pitkänen, J., Iversen, B. V, Douglas, J.T., Paz, A., 2000. Predicting depressional storage from soil surface roughness. Soil Science Society of America Journal 64(5), 1749–1758.
Lehrsch, G.A., Whisler, F.D., Römkens, M.J.M., 1988. Spatial variation of parameters describing soil surface roughness. Soil Science Society of America Journal 52(2), 311–319.
Liang, Z., Feng, Z., Guangxiang, X., 2012. Comparison of Fractal Dimension Calculation Methods for Channel Bed Profiles. Procedia Engineering 28, 252–257.
Linden, D.R., Van Doren, D.M., Allmaras, R.R., 1988. A model of the effects of tillage-induced soil surface roughness on erosion, in: ISTRO 11th Intern. Conference: Tillage and Traffic in Crop Production, Edinburgh, Scotland. pp. 373–378.
Linden, D.R., Van Doren Jr, D.M., 1986. Parameters for characterizing tillage-induced soil surface roughness. Soil Science Society of America Journal 50(6), 1560–1565.
Liu, H.H., Molz, F.J., 1996. Discrimination of fractional Brownian movement and fractional Gaussian noise structures in permeability and related property distributions with range analyses. Water Resources Research 32(8), 2601–2605.
Magunda, M.K., Larson, W.E., Linden, D.R., Nater, E.A., 1997. Changes in microrelief and their effects on infiltration and erosion during simulated rainfall. Soil Technology 10(1), 57–67.
Malinverno, A., 1990. A simple method to estimate the fractal dimension of a self-affine series. Geophysical Research Letters 17(11), 1953–1956.
Mandelbrot, B.B., 1977. Fractals.
Moreira, J.G., Da Silva, J.K.L., Kamphorst, S.O., 1994. On the fractal dimension of self-affine profiles. Journal of Physics A: Mathematical and General 27(24), 8079–8089.
Moreno, R.G., Álvarez, M.C.D., Alonso, A.T., Barrington, S., Requejo, A.S., 2008. Tillage and soil type effects on soil surface roughness at semiarid climatic conditions. Soil and Tillage Research 98(1), 35–44.

Mushkin, A., Gillespie, A.R., 2005. Estimating sub-pixel surface roughness using remotely sensed stereoscopic data. Remote Sensing of Environment 99(1-2), 75–83.
Ogilvy, J.A., Foster, J.R., 1989. Rough surfaces: gaussian or exponential statistics? Journal of Physics D: Applied Physics 22(9), 1243–1251.
Pardini, G., 2003. Fractal scaling of surface roughness in artificially weathered smectite-rich soil regoliths. Geoderma 117(1-2), 157–167.
Paz-Ferreiro, J., Bertol, I., Vidal Väzquez, E., 2008. Quantification of tillage, plant cover, and cumulative rainfall effects on soil surface microrelief by statistical, geostatistical and fractal indices. Nonlinear Processes in Geophysics 15(4), 575–590.
Planchon, O., Esteves, M., Silvera, N., 1998. Micro-relief induced by ridging: Measurement, modelling, consequences on overland flow and erosion. p. 1-7. Poster no. 447. In Proc. 16th World Congress Soil Science. Montpellier, France.
Römkens, M.J.M., Wang, J.Y., 1986. Effect of tillage on surface roughness. Transactions of the American Society of Agricultural Engineers 29(2), 429–433.
Saleh, A., 1993. Soil roughness measurement: chain method. Journal of Soil & Water Conservation 48(6), 527–529.
Skriver, H., 2007. Signatures of polarimetrie parameters and their implications on land cover classification, in: International Geoscience and Remote Sensing Symposium (IGARSS). pp. 4195–4198.
Smith, M.W., 2014. Roughness in the Earth Sciences. Earth-Science Reviews 136, 202–225.
Swain, P.H., King, R.C., 1973. Two effective feature selection criteria for multispectral remote sensing. LARS Technical Reports. Paper 39. 536–540.
Taconet, O., Ciarletti, V., 2007. Estimating soil roughness indices on a ridge-and-furrow surface using stereo photogrammetry. Soil and Tillage Research 93(1), 64–76.
Ulaby, F.T., Moore, R.K., Fung, A.K., 1982. Microwave remote sensing: active and passive. Volume II. Radar remote sensing and surface scattering and emission theory.
Vázquez, E. V, Vieira, S.R., De Maria, I.C., González, A.P., 2009. Geostatistical analysis of microrelief of an Oxisol as a function of tillage and cumulative rainfall. Scientia Agricola 66(2), 225–232.
Verhoest, N.E.C., Lievens, H., Wagner, W., Álvarez-Mozos, J., Moran, M.S., Mattia, F., 2008. On the soil roughness parameterization problem in soil moisture retrieval of bare surfaces from synthetic aperture radar. Sensors 8(7), 4213–4248.
Vermang, J., Norton, L.D., Baetens, J.M., Huang, C., Cornelis, W.M., Gabriels, D., 2013. Quantification of soil surface roughness evolution under simulated rainfall. Transactions of the ASABE 56(2), 505–514.
Vidal Vázquez, E., Miranda, J.G. V, González, A.P., 2007. Describing soil surface microrelief by crossover length and fractal dimension. Nonlinear Processes in Geophysics 14(3), 223–235.
Vidal Vázquez, E., Vivas Miranda, J.G., Paz González, A., 2005. Characterizing anisotropy and heterogeneity of soil surface microtopography using fractal models. Ecological Modelling 182(3-4), 337–353.
Vivas Miranda, J.G., Paz González, A., Rubio, J.L., Morgan, R.P.C., Asins, S., Andreu, V., 2002. Fractal models for the description of soil surface roughness, in: Man and Soil at the Third Millennium. Proceedings International Congress of the European

Society for Soil Conservation, Valencia, Spain. Volume 2. GEOFORMA Edicions, SL, pp. 2099–2112.
Xingming, Z., Kai, Z., Xiaojie, L., Yangyang, L., Jianhua, R., 2014. Improvements in farmland surface roughness measurement by employing a new laser scanner. Soil and Tillage Research 143, 137–144.
Zhixiong, L., Nan, C., Perdok, U.D., Hoogmoed, W.B., 2005. Characterisation of soil profile roughness. Biosystems Engineering 91(3), 369–377.
Zobeck, T.M., Onstad, C.A., 1987. Tillage and rainfall effects on random roughness: A review. Soil and Tillage Research 9(1), 1–20.
Zribi, M., Dechambre, M., 2003. A new empirical model to retrieve soil moisture and roughness from C-band radar data. Remote Sensing of Environment 84(1), 42–52.

Table 1. Description of the different roughness classes triggered by agricultural treatments.

Tillage class	Acronym	Profiles	Description
Mouldboard Plough	MP	20	Tillage operation performed with a plough with multiple mouldboards at a depth of 15-20 cm, resulting in soil inversion and a very rough surface
Harrowed Rough	HR	43	Operation performed normally with a tine harrow to break soil clods and provide a smoother surface suitable for seeding
Harrowed Smooth	HS	29	In cases where the first harrowing did not smoothen sufficiently the surface a second harrowing is applied
Planted Unmodified	PU	44	Seeding operation performed with conventional sowing machinery, normally seed drills
Planted Modified	PM	28	Planted soils modified by the action of the precipitation during 4 months (~250 mm)

Table 2. Summary of roughness parameters analysed.

Type	Parameter	Description	Reference
Vertical	*s (cm)*	Standard deviation of the heights	Allmaras et al., 1966
	LD (cm)	Limiting elevation difference	Linden and Van Doren, 1986
	Sill (cm^2)	Sill of the semivariogram	Croft et al., 2013
	MI (cm)	Microrelief index	Römkens and Wang, 1986
Horizontal	l_{ACF} *(cm)*	Correlation length	Ulaby et al., 1982
	$\rho'(0)$	Initial slope of the auto-correlation function	Ulaby et al., 1982
	LS	Limiting slope	Linden and Van Doren, 1986
	Range (cm)	Range of the semivariogram	Croft et al., 2013
	F (cm^{-1})	Peak frequency	Römkens and Wang, 1986
Combined	Z_S *(cm)*	Combined parameter	Zribi and Dechambre, 2003
	Q ($cm^{1/2}$)	Combined parameter	Linden et al., 1988
	MIF	Combined parameter	Römkens and Wang, 1986
	MUD (cm)	Mean Upslope Depression index	Hansen et al., 1999
	T_S	Tortuosity	Saleh et al., 1993
Fractals	D_{SMV}	Fractal dimension (“semivariogram” method)	Vidal Vázquez et al., 2005
	D_{RMS}	Fractal dimension (“root mean square” method)	Vidal Vázquez et al., 2005
	D_{BC}	Fractal dimension (“box counting” method)	Gneiting et al., 2012
	D_{PS}	Fractal dimension (“power spectrum” method)	Gneiting et al., 2012
	D_{RS}	Fractal dimension (“rescaled range” method)	Liu and Molz, 1996
	l_{SMV} *(cm)*	Crossover length (“semivariogram” method)	Vidal Vázquez et al., 2005
	l_{RMS} *(cm)*	Crossover length (“root mean square” method)	Vidal Vázquez et al., 2005

Table 3. Separability (D_{JM}) of the parameters per pairs of roughness classes. The parameter with the highest separability is in dark grey, and the other two parameters with a high separability for each pair of classes in pale grey.

Parameter	Separability between classes										
	PM-PU	PM-HS	PM-HR	PM-MP	PU-HS	PU-HR	PU-MP	HS-HR	HS-MP	HR-MP	Mean
s (cm)	0.23	1.03	1.61	1.84	0.64	1.33	1.75	0.28	1.24	0.80	1.07
LD (cm)	0.40	1.61	1.67	1.92	0.72	1.25	1.81	0.73	1.64	0.80	1.26
Sill (cm^2)	0.27	1.07	1.45	1.68	0.73	1.25	1.59	0.27	1.16	0.87	1.03
MI (cm)	0.20	0.99	1.58	1.82	0.60	1.29	1.73	0.27	1.23	0.81	1.05
l_{ACF} *(cm)*	0.09	0.08	0.17	0.73	0.01	0.02	0.52	0.03	0.58	0.46	0.27
$\rho'(0)_{ACF}$	0.40	0.09	0.11	1.00	0.15	0.82	1.66	0.34	1.11	0.83	0.65
LS	0.90	1.38	1.47	1.70	0.11	0.16	0.29	0.01	0.06	0.04	0.61
Range (cm)	0.05	0.08	0.27	0.17	0.01	0.16	0.13	0.12	0.11	0.08	0.12
F (cm^{-1})	0.02	0.43	0.59	1.19	0.58	0.78	1.41	0.28	0.76	0.21	0.62
Z_S *(cm)*	0.69	1.26	1.44	1.83	0.24	0.71	1.39	0.37	0.98	0.21	0.91
Q ($cm^{1/2}$)	0.65	1.67	1.75	1.97	0.50	0.96	1.69	0.40	1.36	0.51	1.15
MIF	0.22	0.81	1.37	1.73	0.43	0.98	1.60	0.17	1.06	0.75	0.91
MUD (cm)	0.49	1.65	1.74	1.96	0.64	1.19	1.83	0.58	1.59	0.73	1.24
T_S	0.74	1.58	1.72	1.92	0.38	0.63	1.14	0.10	0.50	0.17	0.89
D_{SMV}	0.34	0.11	0.65	1.59	0.41	1.04	1.74	0.27	1.15	0.50	0.78
D_{RMS}	0.24	0.12	0.90	1.72	0.56	1.30	1.85	0.51	1.47	0.50	0.92
D_{BC}	0.38	0.04	0.59	1.62	0.37	1.11	1.86	0.37	1.35	0.47	0.82
D_{PS}	0.12	0.06	0.75	1.42	0.30	1.12	1.65	0.46	1.16	0.33	0.74
D_{RS}	0.28	0.06	0.15	0.66	0.27	0.81	1.50	0.27	0.95	0.25	0.52
l_{SMV} *(cm)*	0.82	1.61	1.70	1.87	0.38	0.82	1.35	0.35	0.96	0.25	1.01
l_{RMS} *(cm)*	0.85	1.10	1.03	0.93	0.04	0.02	0.01	0.00	0.04	0.02	0.40

Figure list and captions

Figure 1. Examples of surface roughness triggered by agricultural treatments; (A) planted modified by rainfall, (B) planted unmodified, (C) harrowed smooth, (D) harrowed rough and (E) mouldboard plough; and (F) profilometer used for data taking. As a reference, the notebook in C, D, and E is 30 cm long; and 5 m the length of the profilometer bar in F.

Figure 2. Examples of height profiles of each of the roughness classes studied.

Figure 3. Box diagrams per roughness classes of the estimated values of the different parameters.

Figure 4. Spearman correlation matrix of the roughness parameters (n=164).

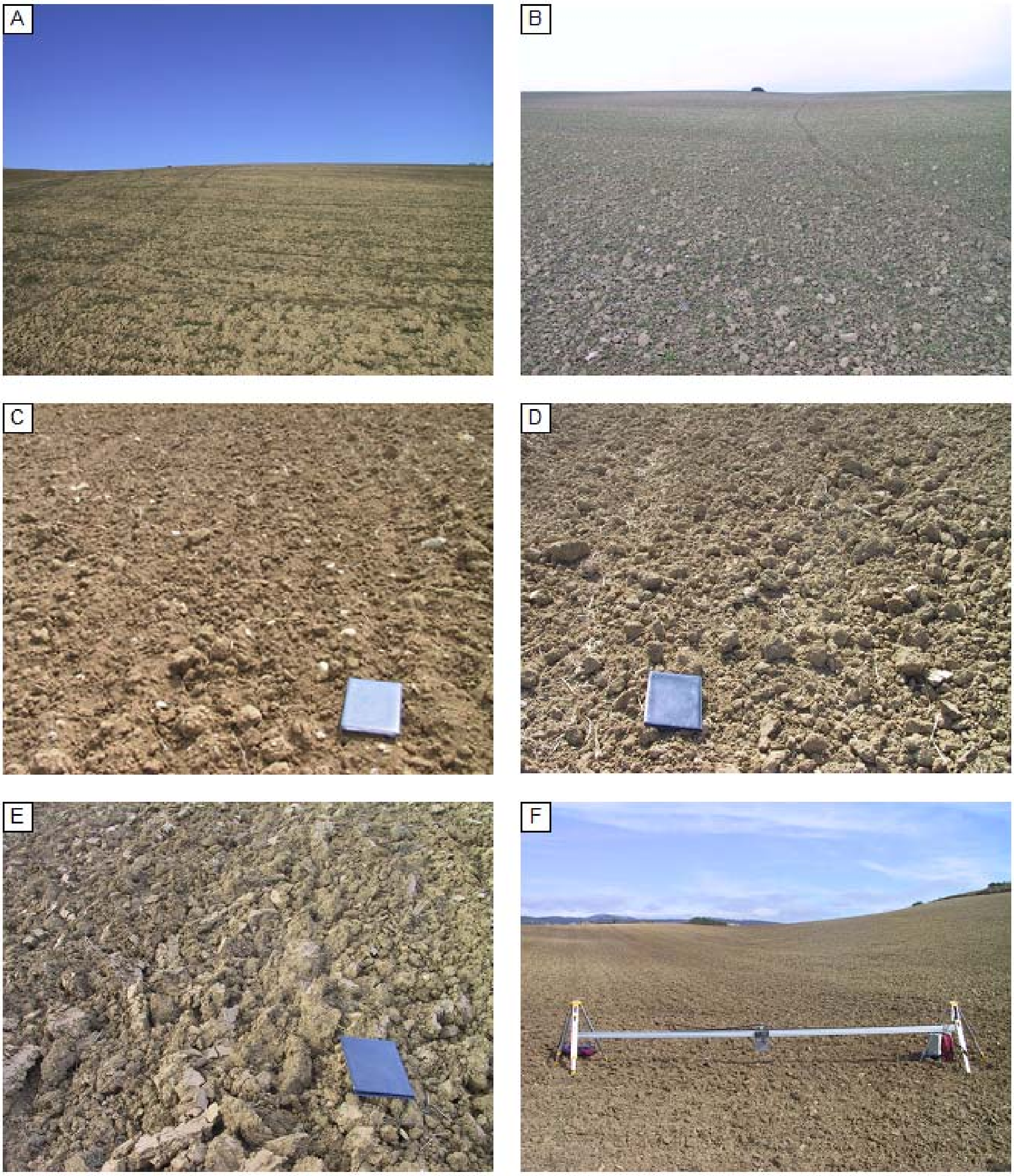

Figure 1. Examples of surface roughness triggered by agricultural treatments; (A) planted modified by rainfall, (B) planted unmodified, (C) harrowed smooth, (D) harrowed rough and (E) mouldboard plough; and (F) profilometer used for data taking. As a reference, the notebook in C, D, and E is 30 cm long; and 5 m the length of the profilometer bar in F.

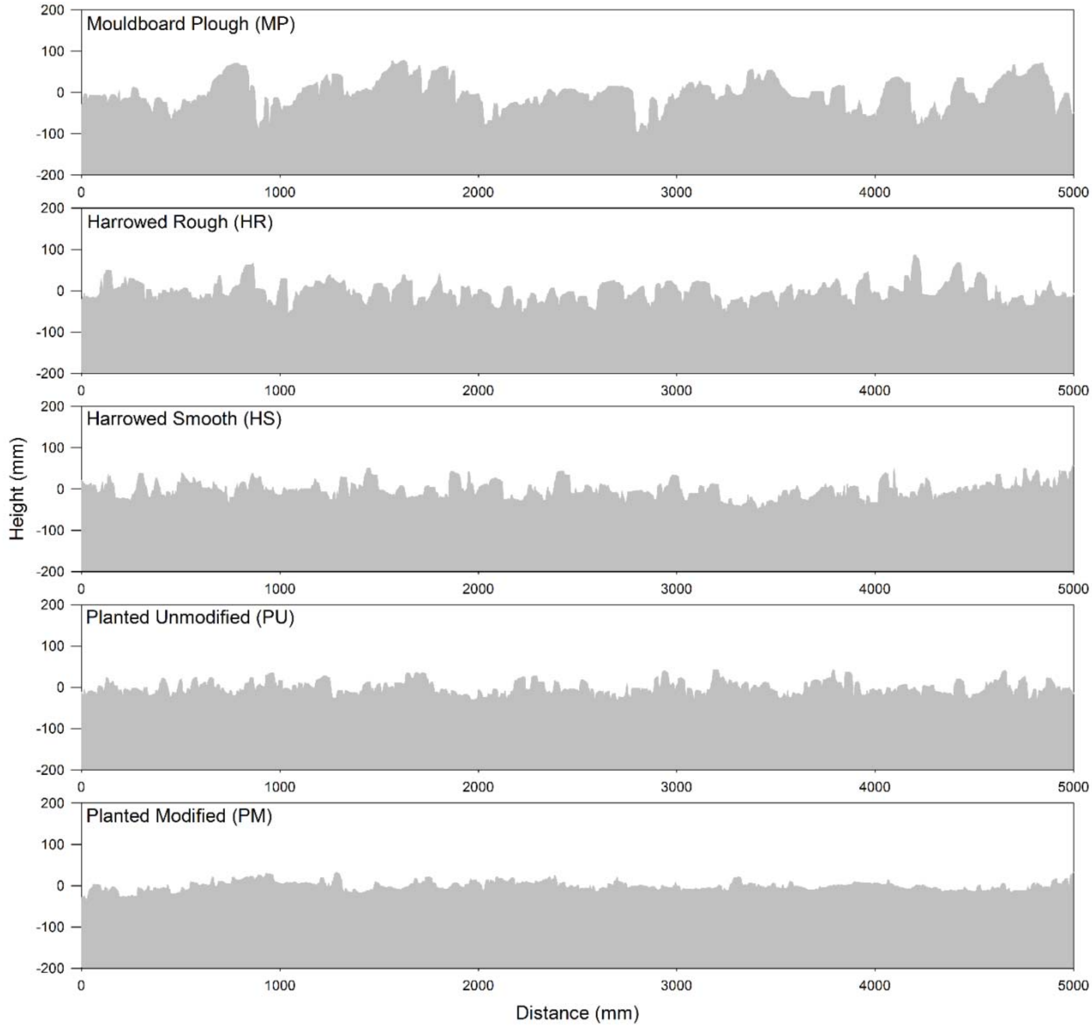

Figure 2. Examples of height profiles of each of the roughness classes studied.

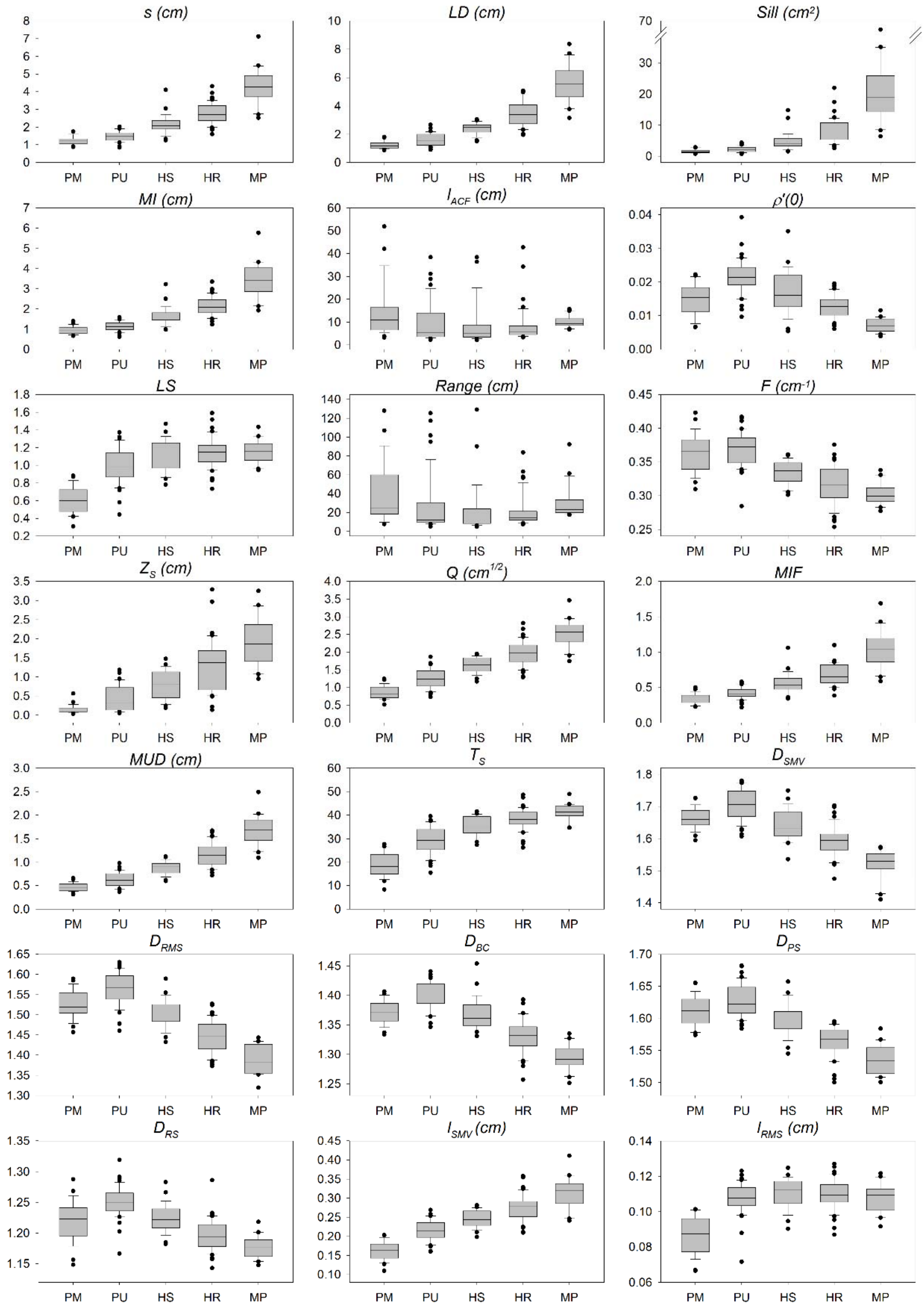

1

2 Figure 3. Box diagrams per roughness classes of the estimated values of the different

3 parameters.

4

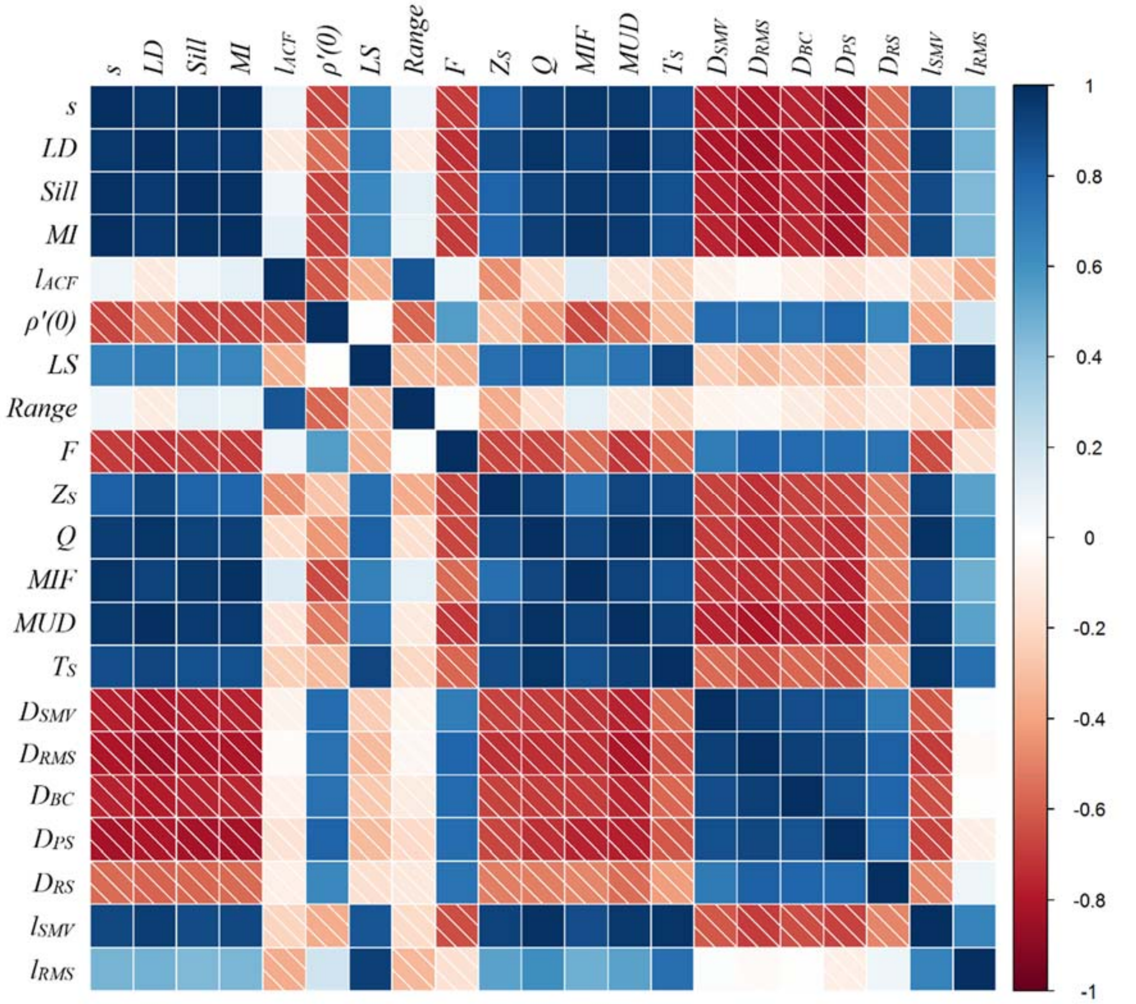

Figure 4. Spearman correlation matrix of the roughness parameters (n=164).